

# STATUS OF THE CNRS-LCSR PROGRAM ON HIGH PRESSURE DROPLET

## VAPORIZATION AND BURNING

N 93 - 20215

Christian Chauveau and Iskender Gökalp  
Centre National de la Recherche Scientifique  
Laboratoire de Combustion et Systèmes Réactifs  
45071 Orléans cedex 2, France

### Introduction

Depending on the surrounding flow and thermodynamic conditions, a single droplet may experience several gasification regimes, ranging from the envelope flame regime to pure vaporization. In practical situations, such as rocket propulsion or diesel combustion, the size distribution of droplets is, at best, bimodal, so that the possibility exists for the simultaneous presence of various regimes. For example, very small droplets are transported by the gas phase with zero relative velocity. This picture validates then the spherical symmetry hypothesis applied to the droplet and to the diffusion flame enveloping it. On the other hand, for larger droplets, a relative velocity exists due to drag forces. The most important influence of forced convection on droplet burning is the possibility to extinguish globally the envelope flame, or to establish a flame stabilized in the wake region. The burning rates of these regimes differ strongly. The characteristic time of droplet gasification is also influenced by the surrounding pressure and temperature. A parametric investigation of single droplet burning regimes is then helpful in providing the necessary physical ideas for sub-grid models used in spray combustion numerical prediction codes.

The CNRS-LCSR experimental program on droplet vaporization and burning deals with these various regimes: stagnant and convective monocomponent droplet burning (refs. 1 and 2); convective mono and bicomponent droplet vaporization (refs. 3 and 4); high temperature convective mono and bicomponent droplet vaporization (ref. 5); burning regimes of hydrazine and hydroxyl-ammonium-nitrate based monopropellant droplets and the vaporization regimes of liquid oxygen droplets. Studies on interacting droplets and on liquid aluminium droplets will start in the near future. The influence of high pressure is a common feature of all these studies. This paper summarizes the status of the CNRS-LCSR program on the effects of high pressure on monocomponent single droplet burning and vaporization, and some recent results obtained under normal and reduced gravity conditions with suspended droplets are presented. In the work described here, parabolic flights of an aircraft is used to create a reduced gravity environment of the order of  $10^{-2}$  g.

### Description of the experimental techniques

#### *The High Pressure Droplet Burning Facility*

Droplet burning experiments under stagnant and variable pressure conditions are performed in a specially designed facility: High Pressure Droplet Burning Facility (HP-DBF). The HP-DBF is designed to investigate

the gasification regimes of suspended or free-floating droplets under variable pressure conditions, up to 12 MPa. Low pressure droplet burning experiments can also be realized (refs. 6, 7 and 8). HP-DBF can be used during the parabolic flights of an aircraft. This apparatus is articulated around a cylindrical combustion chamber of 11 litres capacity, made of an aluminium alloy (AU4G), and mounted on a support structure with a control panel. Two circular flanges are mounted on the two sidewalls of the octogonally shaped external faces of the chamber. Ten identical openings are positioned on the chamber: two openings on the sidewalls to support the droplet injection and ignition systems, and eight along the octagonal perimeter. Two injection needles are positioned face to face and are connected to an electrical pump, allowing the injection of a fuel amount of 0.5 microliters/min. A droplet is formed between the two retractable injectors. A tiltable ( $d = 0.2$  mm) quartz fibre, mounted on the upper chamber wall, can be positioned between the two needles to hold the droplet in the case of suspended droplet experiments. Depending on the droplet burning experiment type, various ignition systems are used. During normal pressure experiments, the droplet is ignited by one pair of electrodes mounted around one injection needle. The ignition spark is produced by a high tension (10 kV) solenoid under 24 V DC. For high pressure droplet burning experiments, an improved version of the injection system and a heated coil for ignition are used. The sequence of injection and ignition operations is computer controlled

### *Diagnostics*

The principle diagnostic systems we are using are based on the visualization of the droplet vaporization or burning phenomena. For droplet burning experiments, the recording equipment is composed of two systems. A high speed video camera, Kodak-Ektapro 1000, which can record up to 1000 full frames per second, allows detailed analysis of droplet burning. The Ektapro 1000 Motion Analyzer's live, real-time viewing makes possible to follow the investigated phenomena frame per frame. A standard video camera, Sony 8 mm PAL, is used to record the droplet and the flame in true colours, but only at 25 frames per second. A second camera has been added to the Kodak-Ektapro 1000 system, in order to be able to observe simultaneously the droplet and the flame with respective appropriate magnification rates. The digitized images from the Ektapro system are transferred to a microcomputer where the image analyses are performed. Details of the image analysis are fully documented in ref. 6.

For droplet vaporization experiments a different imaging system is used. It is composed of a camera, a data acquisition interface, a time base corrector, a micro-computer, and a TV monitor. The camera is monochromatic and has 256 grey levels and a CCD matrix of  $512 \times 512$  pixels. It is equipped with an electronic shutter with a maximum rate of 1/10000. The camera optics provides a maximum magnification rate of 80. The image digitization is done through of a MATROX PIP 1024 interface (video memory 1 Mo) which allows the digitization of an image of  $1024 \times 1024$  or four images of  $512 \times 512$ . A digital time corrector with 1 ms resolution is added. The digitization rate is 50 Hz. Each pixel is coded on 8 bits, that is 256 levels of grey. The microcomputer has a I486DX 33 MHz processor, a hard disk of 200 Mo, 4 Mo of memory and a S-VGA screen.

Suspended droplets are backlighted: this provides the necessary contrast for direct threshold definition. The time to extract the droplet contour is less than 1/50 s to allow the maximum image acquisition rate (50 Hz). The droplet contour determination is based on dichotomic point research methodology. To optimize the speed of frame grabbing and the size of the image data, we have chosen to take only eighty points along the contour. These data are simultaneously memory saved and displayed on the screen. At the end of the acquisition (750 frames) the complete data sets are transferred to the hard disk. The data analysis consists in calculating the surface area from the contour points and to obtain the droplet equivalent diameter. The droplet diameter and its corresponding time are saved in a synthesized file. The major advantage of the method is its well defined time resolution, characterized by the impressive number of pictures taken into account during a droplet lifetime.

## Results and discussion

### *High pressure low temperature vaporization experiments*

Preliminary experiments have been conducted under normal gravity conditions to determine the influence of ambient pressure on the vaporization of n-heptane and methanol droplets in air at 300 K (or  $T_r = T/T_c = 0.56$  and 0.59 respectively). The maximum reduced pressure  $P_r = P/P_c$  was 3.6 for heptane and 1.2 for methanol. Droplet initial diameters were between 1 mm and 1.5 mm. The variation with time of  $(d/d_0)^2$  for n-heptane droplets is shown on Fig. 1. These curves are used to determine an average vaporization constant,  $K_{av}$ . The variation of  $K_{av}$  with  $P/P_c$  is shown on Fig. 2.  $K_{av}$  decreases strongly for  $P/P_c < 1$  and shows a weakly increasing behaviour for  $P/P_c > 1$ . The decrease of  $K_{av}$  for  $P/P_c < 1$  can be explained by the increased ambient gas density which delays the build up of the fuel vapour concentration profile near the droplet surface and its further diffusion into the ambience. The decrease of  $K_{av}$  in the subcritical pressure regime is confirmed by methanol droplet vaporization experiments (Fig. 2). They also show another phenomenon for moderate pressures. The data for pure methanol for  $P = 0.1$  MPa indicates a sequential vaporization behaviour (Fig 3). This behaviour is no more observed for approximately  $P/P_c > 0.3$ . The sequential vaporization behaviour of methanol droplets for moderate pressures is to be compared with the observations of refs. 9 and 10. The curves of  $d^2(t)$  are also used to determine the instantaneous vaporization rates (Figs. 4a and 4b). For heptane droplets, the largest variation is observed for the atmospheric pressure case. For increasing pressures,  $K(t)$  increases during the last quarter of the vaporization lifetime, which may well be an artefact of the influence of the suspension fibre. Except the moderate pressure experiments,  $K(t)$  for methanol droplets shows the same behaviour. A quasi-steady state process can thus be assumed to characterize high pressure vaporization of n-heptane and methanol droplets in room temperature air.

### *High pressure droplet burning experiments*

High pressure burning experiments have been conducted with n-heptane and methanol droplets. The experiments with n-heptane droplets were conducted under reduced gravity conditions only up to a maximum pressure of 0.65 MPa. With increasing pressure, they show (ref. 10) a gradual increase of the average burning rate and an increasing non-stationary behaviour of the instantaneous burning rate. n-heptane burning droplet experiments have been continued for higher pressures under normal gravity. Contrary to the results of ref. 11, the vanishing surface tension prevented to increase the pressure above 1.8 MPa. The increased soot formation also prevented the determination of the instantaneous droplet diameter. An average burning rate is then determined by assuming the  $d^2$  law and by using the duration of the flame luminosity as the burnout time. The results are presented on Fig. 5 with error estimate margins. The reduced gravity results are clearly lower than the corresponding normal gravity results. The variation with pressure of the average burning rate in the subcritical regime can be represented with a power law of the form  $P^{0.36}$ .

Burning experiments of considerably less sooting methanol droplets have been conducted under reduced gravity conditions to be able to detect the instantaneous droplet diameter. These experiments have been conducted between normal atmospheric pressure and a maximum reduced pressure of  $P_r = 0.63$ . Two pictures of a burning suspended methanol droplet with  $d_0 = 1.5$  mm and for  $P_r = 0.63$  are shown on Plate I. Figure 6 presents the curves of  $d^2(t)$  for two pressures. The sequential gasification behaviour is not observed even for the lowest pressure range (see also ref. 12). As shown on Fig. 7, the average burning rate increases with pressure. Three methods have been compared on this figure: the method based on the  $d^2$  law and the droplet lifetime; the method based on the average slope of the  $d^2(t)$  curve; and that based on the average value of  $K(t)$ . As a first approximation, and for the pressure range investigated here, the three methods give comparable values and a quasi-linear increase of the average burning rate with pressure. Figure 8 shows the instantaneous burning rates for high pressure methanol droplet burning experiments. The curve for the highest pressure,  $P = 5$  MPa, is distinguishable from the others by its accentuated non-stationary behaviour.

### Future work

The investigation of high pressure effects will be the main focus of the future LCSR work on droplet gazification regimes. The supercritical regime will be approached with the help of a new version of the HP-DBF which is under construction: it will allow to increase the temperature as well as the pressure of the ambient medium. This apparatus will be used to investigate the vaporization and burning of mono and multicomponent fuel droplets in high pressure and high temperature conditions and also to compare normal gravity and reduced gravity experiments to infer natural convection effects. An electrodynamic balance is under development and will be added to the apparatus. It will allow to conduct supercritical vaporization experiments under normal gravity conditions. The parabolic flights of the Caravelle aircraft will be continued to be used for suspended droplet experiments. A new high pressure droplet burning module will be developed to be used during sounding rocket experiments in collaboration with ESA/ESTEC and MBB-ERNO. A major purpose of the following years is the investigation of high pressure vaporization of liquid oxygen droplets. A collaboration is established with the University of Marseille and ONERA to develop the numerical modelling part of this task.

### Acknowledgments

The droplet vaporization and burning studies program of the CNRS-LCSR is supported by the Microgravity Office of the European Space Agency, the Centre National d'Etudes Spatiales, the Société Européenne de Propulsion, the Commission of the European Communities, the Joint Research Programme of the European Car Manufacturers, the French Army Research Office, and ONERA.

### References

1. Gökalp, I., Chauveau, C., Richard, J.R., Kramer, M. and Leuckel, W., **Twenty-Second Symposium (International) on Combustion**, The Combustion Institute, Pittsburgh, 1988 pp. 2027-2035.
2. Chauveau, C. and Gökalp, I., **Proceedings of 7th. European Symposium on Materials Sciences and Fluid Physics in Microgravity**, ESA-SP-295, 1990, pp. 467-472.
3. Gokalp, I., Chauveau, C., Simon, O. and Chesneau, X., **Combustion and Flame**, vol. 89, 1992, pp. 286-298.
4. Gokalp, I., Chauveau, C., Ramos-Arroyo, N.A., Berrekam, H. and Chesneau, X., **Proceedings of the 5th ILASS Americas**, May 18-20, 1992, San Ramon, Ca.
5. Ramos-Arroyo, N.A., Berrekam, H., Chauveau, C. and Gökalp, I., Paper to be presented at the **Fall Meeting of the Western States Section of the Combustion Institute**, October 12-13, 1992, Berkeley, Ca.
6. Chauveau, C., Vaporisation et Combustion des Gouttes Isolées de n-Heptane. Etude en Microgravité et Influence de la Convection Forcée. **PhD. Thesis**, Université d'Orléans, 1990
7. Chauveau, C. and Gökalp, I., **Ann. Chim. Fr.**, vol. 17, 1992, pp. 27-44.
8. Chesneau, X., Chauveau, C. and Gökalp, I., **Proceedings of the First European Symposium on Fluids in Space**, ESA SP-353, 1992, pp. 407-418.
9. Law, C.K., Xiong, T.Y. and Wang, C.H., **Int. J. Heat Mass Transfer**, vol. 30, no. 7, 1987, p. 1435.
10. Cho, S.Y., Choi, M.Y. and Dryer, F.L., **Twenty-Third Symposium on Combustion**, The Combustion Institute, 1990, pp. 1611-1617.
11. Sato, J., Tsue, M., Niwa, M. and Kono, M., **Combustion and Flame**, vol. 82, 1990, pp. 142-150.
12. Yang, J.C., Jackson, G.S. and Avedisian, C.T., **Twenty-Third Symposium on Combustion**, The Combustion Institute, 1990, pp. 1619-1625.

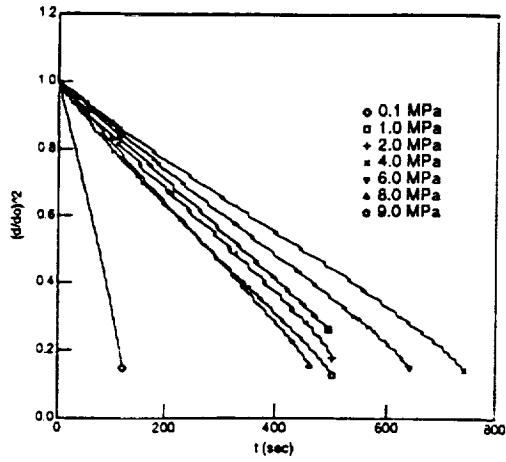


Fig. 1 : Influence of the ambient pressure on the vaporization of n-Heptane droplets.

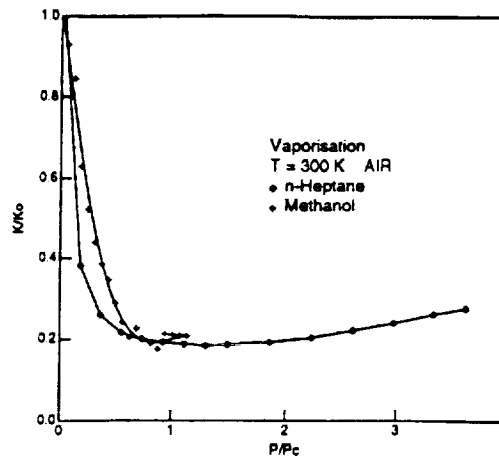


Fig. 2 : Evolution of  $K/K_o$  with  $P/P_c$  for n-Heptane and Methanol droplets.

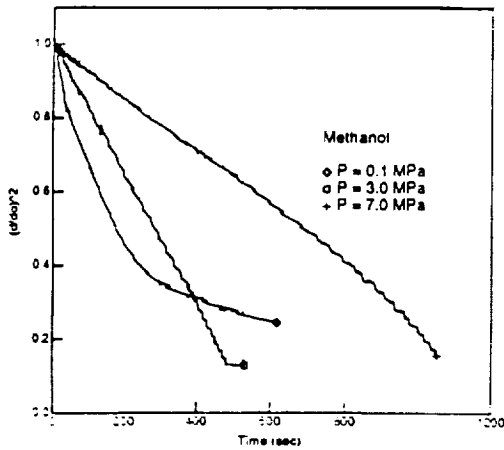


Fig. 3 : Influence of the ambient pressure on the vaporization of Methanol droplets.

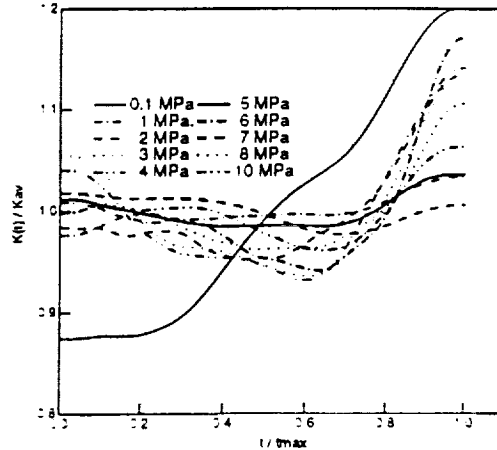


Fig. 4a : Instantaneous vaporization rates for n-Heptane droplets.

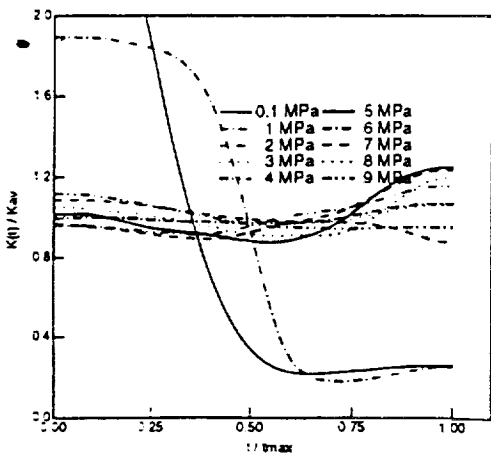


Fig. 4b : Instantaneous vaporization rates for Methanol droplets.

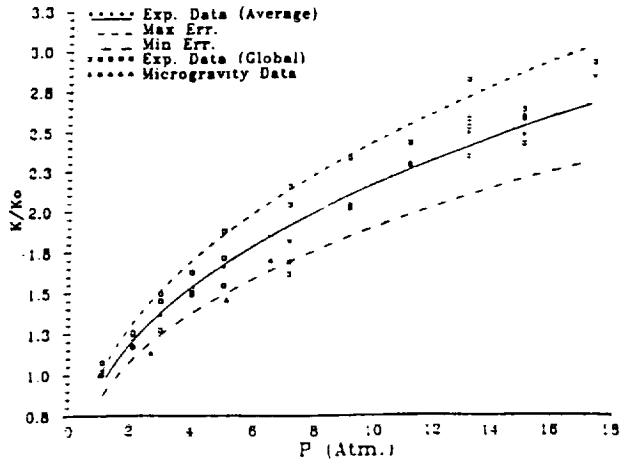


Fig. 5 : Influence of the ambient pressure on the combustion of n-Heptane droplets





(a)  $t = 520$  ms

(b)  $t = 1244$  ms

Plate 1 : Pictures of a burning suspended Methanol droplet;  $P = 5$  MPa,  $g = 10^{-2} g_0$ ,  $d_0 = 1.5$  mm

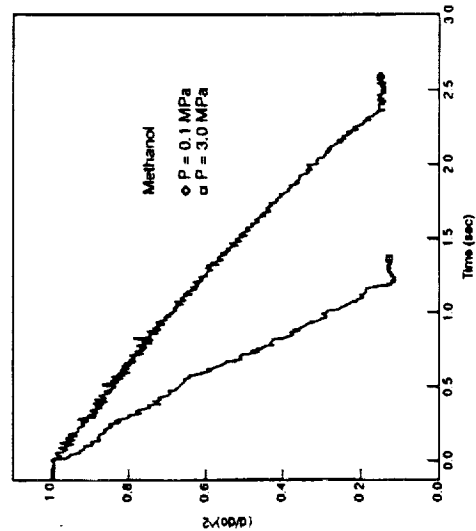


Fig. 6 : Evolution of  $(d/d_0)^2$  with time for Methanol droplet burning in microgravity.

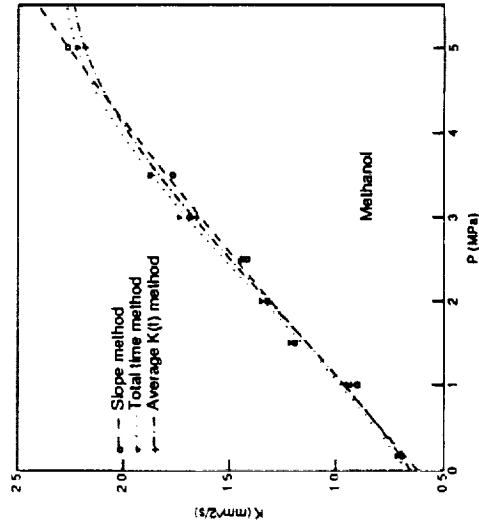


Fig. 7 : Evolution of the average burning rate with the ambient pressure, for Methanol droplets, in microgravity.

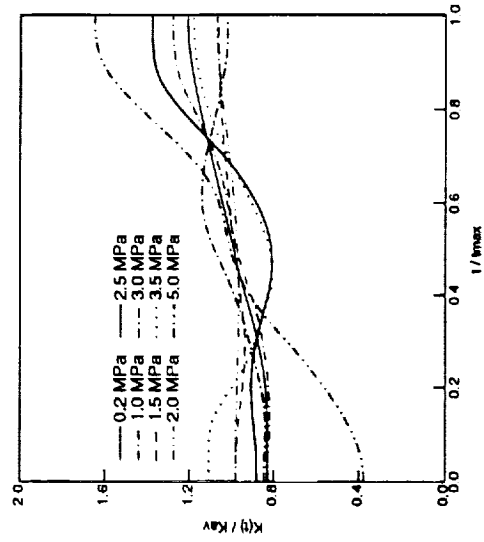


Fig. 8 : Instantaneous burning rate for high pressure methanol droplet burning experiments.

